RSC Advances

PAPER

View Article Online
View Journal | View Issue

Cite this: *RSC Adv.*, 2022, **12**, 8137

Electrochemical preparation of monodisperse Pt nanoparticles on a grafted 4-aminothiophenol supporting layer for improving the MOR reaction

Nguyen Tien Hoang,[a] Pham Truong Thuan Nguyen,[b] Pham Do Chung,[c] Vu Thi Thu Ha,[d] Tran Quang Hung,[d] Pham Thi Nam[e] and Vu Thi Thu*[a]

Received 4th January 2022
Accepted 8th March 2022

DOI: 10.1039/d2ra00040g

rsc.li/rsc-advances

The methanol oxidation reaction (MOR) has recently gained a lot of attention due to its application in fuel cells and electrochemical sensors. To enhance the MOR, noble metal nanoparticles should be homogeneously dispersed on the electrode surface with the aid of one suitable support. In this work, 4-aminothiophenol (4-ATP) molecules which contain simultaneously amine and thiol groups were electro-grafted onto the electrode surface to provide anchoring sites, limit aggregation and ensure good dispersion of metal nanoparticles. The results showed a high density of platinum nanoparticles (PtNPs) with an average size of 25 nm on the glassy electrode modified with a 4-ATP supporting layer. Consequently, the MOR was improved by 2.1 times with the aid of the grafted 4-ATP layer. The electrochemical sensor based on PtNPs/4-ATP/GCE is able to detect MeOH in a linear range from 1.26 to 21.42 mM with a detection limit of 1.21 mM.

1. Introduction

Pt is an important catalyst for the methanol oxidation reaction (MOR) in direct methanol fuel cells (DMFC)[1,2] and methanol sensors.[3] To maximize the catalytic activity of Pt, it is essential to disperse homogeneously distinct metal nanoparticles (size of several to tens of nanometers) on suitable supports. Carbon materials and conducting polymers are of special interest during the last two decades for their prevention of particle aggregation and good mechanical stability.[2,4] Several conducting polymers such as poly-*o*-aminophenol,[4] polyaniline (PANI),[5] polypyrrole (PPy),[6,7] poly(3,4-ethylenedioxythiophene) (PEDOT),[8] *etc.* have been demonstrated to provide large surface areas for deposition of metal nanoparticles and be able to cover surface defects which are harmful for dispersion of metal particles.[4] Furthermore, the presence of such a supporting matrix might also promote the nucleation of a high density of small particles,[8] increase the electrical percolation of metal nanoparticles, and possibly increase the electrical conductivity in the composite *via* synergistic transport with Pt nanoparticles.[6] More importantly, the presence of these organic matrices can also enhance the oxidation rate of undesired oxidative intermediates (known as CO_{ads}) which are considered to be the origin of the CO poisoning effect.[8] It is worthy to notice that there is always an abundant number of S or N atoms in the above polymeric films. It was also reported that the presence of S or N heteroatoms in carbon supports might also enhance stability of Pt nanoparticles since they can provide more binding sites to firmly immobilize metal particles.[9,10] Evenly, the introduction of such heteroatoms probably increase local charge and spin density of carbon atoms in the carbon supporting layer and make them become an alternative catalyst[11] which sometime might be comparable with Pt.[12] Otherwise, it was also found that thiolization of carbon supports[13] might be able to shift binding energy of Pt to higher values which are favorable for electro-catalytic reactions; whereas hydroxylation of carbon supports[14] enables CO anti-poisoning property by facilitating oxidative removal of intermediates in MOR.

Currently, (4-aminothiophenol) (4-ATP) – an aromatic compound containing both amine and thiol functional groups – has first been utilized to generate monodisperse Pd nanoparticles for ethanol oxidation reaction.[15] It was suggested that the high density of locally adsorbed OH^- on grafted 4-ATP supporting layers is responsible for promoting anti-poisoning behavior and catalytic activity at electrode surfaces. Historically, 4-ATP was often used as a bi-functional ligand to construct hybrid nanostructures[16] or fix biomolecules (*i.e.*, antibodies, cells) onto electrode surfaces.[17] The electrodeposited 4-ATP film has also been utilized as a matrix for immobilization of biomolecules in biosensing applications.[18] Monodisperse gold nanoparticles can be

[a]*University of Science and Technology of Hanoi (USTH), Vietnam Academy of Science and Technology (VAST), 18 Hoang Quoc Viet, Cau Giay, Hanoi, Vietnam. E-mail: thuvu.edu86@gmail.com; vu-thi.thu@usth.edu.vn*

[b]*CY Cergy Université, LPPI, F-95000 Cergy, France*

[c]*Hanoi National University of Education (HNUE, 134 Xuan Thuy, Cau Giay, Hanoi, Vietnam*

[d]*Institute of Chemistry (IOC), Vietnam Academy of Science and Technology (VAST), 18 Hoang Quoc Viet, Cau Giay, Hanoi, Vietnam*

[e]*Institute of Tropical Technology (ITT), Vietnam Academy of Science and Technology (VAST), 18 Hoang Quoc Viet, Cau Giay, Hanoi, Vietnam*

achieved by combining electro-polymerization of self-assembled 4-ATP molecules on gold electrodes with electrodeposition of metal particles.[19] Deposition of a thin 4-ATP layer on top of gold nanostructures might help to improve peak separation in electrochemical simultaneous detection of redox species.[20] The 4-ATP material if co-electrodeposited with gold nanoparticles was demonstrated to be a good matrix to disperse them with very limited aggregation due to presence of thiol group.[21,22]

Electrochemical deposition is an effective method for the preparation of metal nanoparticles with controllable morphology and density which are crucial for their good dispersion and high catalytic activity. Direct electro-deposition generally leads to three-dimensional growth of Pt nanoparticles on electrode surfaces,[4,23,24] but also possibly create metallic monolayer or controllable multilayer films if needed.[25–27] Especially, alloying Pt with other metals (Au, Ni Co, Cu) can be easily and quickly achieved *via* electrochemical approach without using hazardous agents.[28]

In this work, we have prepared monodisperse Pt nanoparticles on a very thin 4-ATP supporting layer using electrochemical approach for further applications in MOR reaction. The effect of synthesis conditions on MOR signal was investigated. The growth mechanism of 4-ATP film and its role in enhanced MOR effect will be also discussed.

2. Experimental

2.1. Materials and apparatus

4-Aminothiophenol (4-ATP, 97%), chloroplatinic acid ($H_2PtCl_6 \cdot xH_2O$), Lithium perchlorate ($LiClO_4$, 98%), methanol (MeOH, anhydrous, 99.8%) were purchased from Sigma-Aldrich. All electrochemical experiments were conducted on an Autolab potentiostat (Metrohm, Netherland) by using three-electrode cell in which (modified) glassy carbon electrodes (GCE) were used as working electrode, Ag/AgCl electrode as reference electrode and Pt wire as counter electrode. The morphology of all samples were visualized under scanning electron microscopy (SEM) (Hitachi S-4800) operated at 5 kV acceleration voltage.

2.2. Preparation of clean glassy carbon electrode

The cleaning step is essential for eliminating the contamination on the surface of working electrode. This preparation was performed by gentle polishing glassy carbon electrode (GCE) on a polishing pad impregnating with 0.3 μm alumina/water slurry followed by thoroughly washing with distilled water. The procedure is repeated until a mirror-look electrode surface is obtained. The electrode surface was then verified by sweeping the potential from −1.2 V to 1.2 V *vs.* Ag/AgCl electrode for several cycles in 0.5 M H_2SO_4 solution by means of cyclic voltammetry (in which redox signals of Pt and *p*-ATP might occur). The GCE was finally rinsed with distilled water and dried at room temperature until use.

2.3. Electro-grafting 4-ATP on GCE

The electrochemical deposition of 4-ATP was realized by performing 2 consecutive cyclic cycles with a staircase from −0.1 to 1.25 V at a scan rate of 50 mV s^{-1} in deaerated 0.1 M $LiClO_4$ ethanolic solution containing 5 mM 4-ATP. After the electrodeposition process, the 4-ATP/GCE electrode was rinsed gently with distilled water and dried at room temperature. We have chosen ethanol as solvent for deposition of 4-ATP layer to ensure the solubility of 4-ATP molecules.

2.4. Electrodeposition of PtNPs on 4-ATP/GCE

The electrodeposition of Pt nanoparticles was performed by sweeping 4-ATP/GCE electrode in deaerated aqueous solution containing 1 mM H_2PtCl_6 and 0.1 M KCl with staircase of 0.1 V to −1.25 V for 2 cycles at a scan rate of 50 mV s^{-1}. The modified electrode was rinsed with distilled water and dried naturally at ambient conditions.

2.5. MOR test

Methanol oxidation reaction (MOR) in alkaline condition (0.5 M NaOH) was tested by cyclic voltammetry method. The cyclic voltammograms were recorded for 1 cycle at potentials from −0.8 to 0.2 V at scan rate of 50 mV s^{-1}. The forward and backward currents were calculated to investigate catalytic activity of modified electrode.

3. Results and discussions

3.1. Electro-grafting of thin 4-ATP supporting layer on GCE

The cyclic voltammogram recorded during electro-grafting of 4-ATP layer was shown in Fig. 1. In the first cycle, an anodic peak appeared at +920 mV (*vs.* Ag/AgCl) is probably attributed to the oxidation of 4-ATP molecules into aminyl radicals which are rapidly attached into electrode surface.[21,29] In the second cycle, one redox pair relevant to grafted 4-ATP material occurred at +340 mV/+520 mV which are in agreement with observations obtained in previously reported works.[15,19] By increasing the number of CV cycles, the peak current decreases as well as the peak-to-peak separation increases, thus, blocking effect was also observed as the thickness of the film increases. In absence of mobile proton in the medium, the electro-polymerization of 4-ATP could have hardly occurred after only several scan cycles, leading to the formation of thin film of this compound. Afterwards, the deposition conditions are optimal at precursor concentration of 5 mM, scan rate of 50 mV s^{-1}, and number of scans of 2. The deposition mechanism of 4-ATP thin film can be proposed as follows. The precursor molecules are initially attracted towards electrode surface, and then spontaneously grafted on the electrode surface through oxidation of amine functional group to form their corresponding cationic radicals which subsequently make linkage with carbon atoms on electrode surface.[29]

According to cumulated charges deliver during deposition, the surface concentration of resulted layer is calculated about 2.8 nmol cm^{-2} which corresponds to a thickness of 4.5 nm by assuming that the 4-ATP layer is fully compacted ($\Gamma_{monolayer}$ ~0.5 nmol cm^{-2}) and the thickness of the monolayer is 8 Å.[30,31] With increasing in deposition cycles, the thickness of the film reaches 9 nm after 10 cycles.

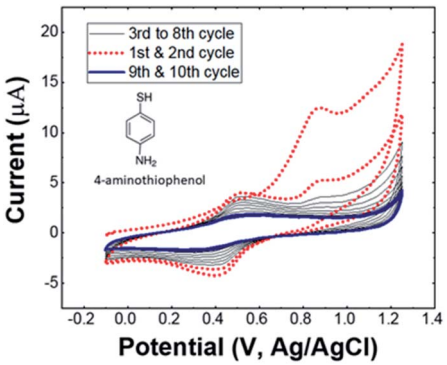

Fig. 1 Cyclic voltammograms recorded during electro-grafting 4-ATP on GCE. Scan rate: 50 mV s^{-1}. Electrolyte: 100 mM $LiClO_4$ in EtOH. $C_{4\text{-ATP}}$ = 5 mM.

3.2. Electrochemical preparation of monodisperse PtNPs on 4-ATP/GCE

Fig. 2 represents cyclic voltammograms recorded during electrodeposition of PtNPs on 4-ATP/GCE. It can be seen that the intensity of reduction peak is relatively weak in the first cycle but becomes significant in the second one. As aforementioned, the presence of 4-ATP layer provokes a blocking effect towards electron transfer of the redox species at the vicinity of the electrode surface, leading to a lowering in nucleation and growth of Pt NPs as displayed for the first cycle, resulting to formation of smaller and well-structured particles. Nevertheless, an oxidation peak was also observed at the reverse scan, which is corresponding to the oxidation of deposited metallic Pt. The onset potential for the deposition of Pt NPs using modified electrode is determined at −0.28 V (*vs.* Ag/AgCl) which is 40 mV more positive than the onset potential of bare GCE. Once the Pt seeds were formed, the Pt NPs are obviously grown from the 2nd cycle, resulting from a reduction peak at −0.59 V.

The overall reduction reaction of $PtCl_6^{2-}$ is a four-electron process:

$$PtCl_6^{2-} + 4\,e^- \rightarrow Pt^0 + 6\,Cl^-$$

The reduction charge can be deduced from the area of reduction peak as:

$$Q_{Pt} = \frac{\int i\mathrm{d}V}{\nu}$$

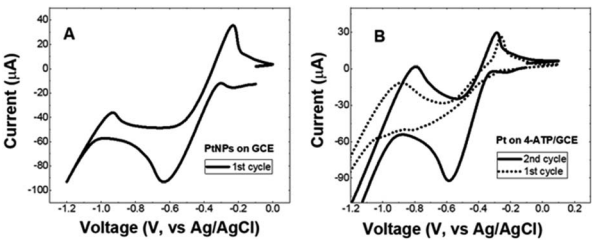

Fig. 2 Electrodeposition of PtNPs on GCE (A) and 4-ATP/GCE (B).

where ν is the scan rate (V s^{-1}) and $\int i\mathrm{d}V$ is the area of reduction peak.

The amount of deposited Pt (m_{Pt}) is obtained as follows:

$$m_{Pt} = \frac{Q_{Pt}M}{4F}$$

where M is the atomic weight of Pt (195.09 g mol^{-1}) and F is the Faraday constant (96 485.309 C mol^{-1}).

The deposition charge observed on 4-ATP modified electrode and bare electrode were estimated to be 288 μC and 286 μC, respectively. Thus, the amount of Pt loaded onto bare and modified electrodes are nearly the same and estimated to be 0.15 μg.

The deposition of PtNPs on electrode surface is basically initiated by nucleation process, and then followed by the growth of metal nuclei. It was reported that the 3D progressive nucleation model is more suitable for the growth of PtNPs on carbon supports (*i.e.*, glassy carbon electrode, mesoporous carbon) or almost organic films.[4,8] Consequently, the metal particles deposited onto 4-ATP modified electrode should be in spherical shape and distributed throughout the entire electrode surface.

3.3. Electrochemical behaviour

Electrochemical behaviour of PtNPs/4-ATP modified electrode was evaluated by cyclic voltammetry (CV) in nitrogen-saturated 0.5 M H_2SO_4 solution at scan rate of 50 mV s^{-1}. An oxidation peak related to hydrogen desorption process on the surface of PtNPs (Fig. 3) was identified at −0.1 V on both PtNPs/GCE and PtNPs/4-ATP/GCE while hydrogen adsorption peak is not clearly observed. In literature, the hydrogen adsorption–desorption process recorded on crystalline Pt nanostructures generally exhibits multiple peaks.[4,32] The reason behind this might be due to the fact that the preferable faces for hydrogen adsorption were not fully exposed to the environment. Consequently, the adsorption kinetics on those facets is relatively low, thus hindered by hydrogen evolution reaction.

The electrochemical active surface area (ECSA) can be deduced from the hydrogen adsorption–desorption process on cyclic voltammogram recorded in acidic solution (Fig. 3).

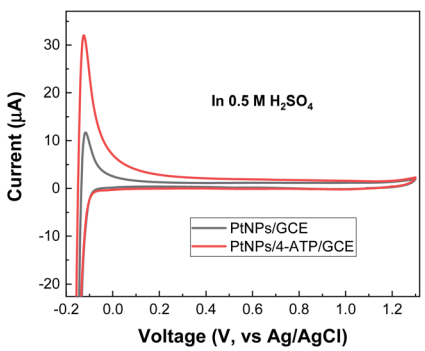

Fig. 3 Electrochemical characterization. Cyclic voltammograms of PtNPs/GCE and PtNPs/4-ATP/GCE recorded in 0.5 M H_2SO_4.

Indeed, the Pt–O stripping peak at higher potentials might be also useful for this but generally less accurate.

It was assumed that 1 cm^2 of smooth Pt required 210 μC for the adsorption of one electron per Pt site.[4,32] Thus:

$$S_{Pt} = \frac{Q_H}{210\ \mu C\ cm^{-2}}$$

where Q_H is estimated from the area of H adsorption–desorption peak as follows:

$$Q_H = \frac{\int i dV}{v}$$

with v is the scan rate (V s^{-1}) and $\int i dV$ is the area of hydrogen adsorption–desorption peak.

The charge of hydrogen adsorption–desorption process (Q_H) and the active surface area (S_{Pt}) were determined to be 69 μC and 0.327 cm^2, respectively. These values are three times higher than those obtained on PtNPs modified GCE (23.1 μC and 0.111 cm^2).

Electrochemical impedance spectra (EIS) of bare and modified GCE electrodes were also investigated (Fig. 4). For bare GCE, one semicircle was obtained at high frequency region whereas a linear line was observed at lower frequencies.[33,34] The diameter of this semicircle is indeed related to the electron transfer resistance at electrolyte–electrode interface. The charge transfer resistance was estimated to be 400 Ohm for bare GCE (fitted using Randles equivalent circuit). Obviously, the diameter of this semicircle was decreased once PtNPs was deposited onto electrode surface and the charge transfer was 70 Ohm for GCE electrode modified with only PtNPs. When the 4-ATP organic layer was grafted onto electrode surface, the EIS spectrum shows a very large semicircle which is a clear evidence for blocking effect (as discussed in Section 3.1). On the other hand, it seems that a monolayer of 4-ATP has been grafted onto electrode surface[35] instead of a thick polymer film as reported in several previous works.[15,19,21] The charge transfer resistance was about 1500 Ohm for PtNPs/4-ATP/GCE electrode. It means that the metal nanoparticles have successfully grown with the aid of 4-ATP supporting layer despite of the low transfer rate at electrode surface.

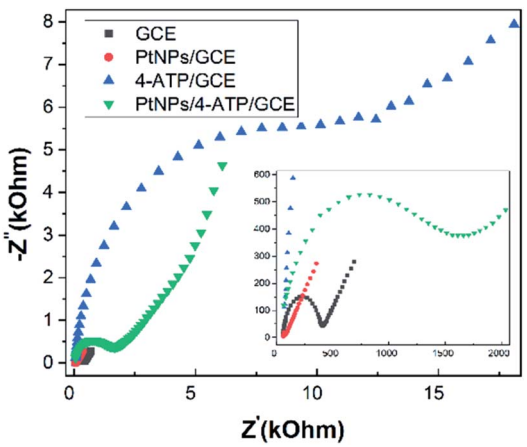

Fig. 4 EIS spectra recorded in 5 mM $Fe(CN)^{3-/4}$ in 100 mM KCl solution.

3.4. SEM images and EDX analysis

SEM images of PtNPs grown on 4-ATP film was captured on flat FTO (fluorine doped tin oxide) electrode for convenience. It can be seen that the metal nanoparticles have been deposited onto 4-ATP modified electrode with higher density and homogeneity (Fig. 5). It seems that the number of nucleation sites was increased whereas the accumulation of grown nanoparticle is significantly limited with the aid of organic supporting film. As suggested, the free thiol functional groups in anchoring layer might have provided more nucleation sites, thus leads to homogeneous distribution of metal nanoparticles on electrode surface.[15,21,32] Also, the entire supporting layer itself is actually a good dam to restrict diffusion of metal ions to electrode surface, slow down their reduction, thus allows us to have a better control in growth process of metal nanoparticles. Similar results were obtained when conventional polymers or carbon supports were used to disperse metal nanoparticles in previously reported works.[5–8] The average size of PtNPs grown on bare FTO electrode and 4-ATP modified FTO electrode is 60 nm and 25 nm, respectively. These results have confirmed again the reduction in particle size in presence of 4-ATP layer as calculated hydrogen adsorption–desorption process.

EDX analysis was also conducted to evaluate the amount of metal nanoparticles. The weight percentage and atomic percentage of platinum element was increased from 0.87% and 0.5% for PtNPs grown on bare FTO to 1.17% and 0.18% for PtNPs grown on 4-ATP modified FTO electrode (Fig. 5). EDX mapping results have shown a homogeneous distribution of S atoms in 4-ATP grafted layer and Pt atoms over the electrode surface (Fig. 5).

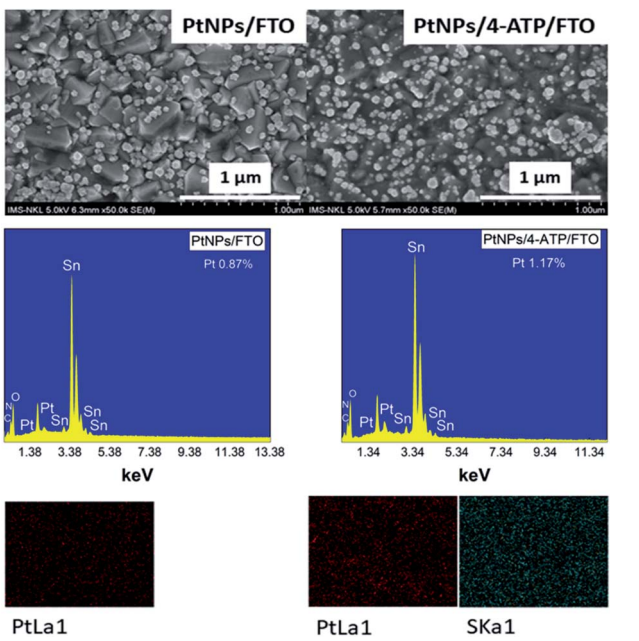

Fig. 5 SEM images and EDX analysis of PtNPs and PtNPs/4-ATP.

3.5. MOR test

The relatively low activation energy (35 kJ mol^{-1}) for electro-sorption of methanol on Pt makes this metal becomes the most effective catalyst for MOR effect.[1] It has been evidenced that the catalytic activity of PtNPs towards MOR is strongly affected by their shape and size, and it was found that the active sites for catalytic activity are normally located at surface defects (steps, kinks).[36–38]

The mechanism of MOR with using Pt as a catalyst has been well-documented (Fig. 6). Typically, the oxidation of methanol is consisted of electro-sorption of methanol on the active sites at the platinum surface[1] followed by its dissociation into different intermediates.[8] These latter are further converted themselves into more firmly adsorbed species, *i.e.* transformation of CHO_{ads} to CO_{ads}. As the electron transfer kinetic of this reaction is relatively high, this process is the main cause of active site's blocking at the surface of platinum, which is so-called poisoning phenomena.[14,39] Therefore, the crutical step in the reaction pathway is the oxidation of adsorbed formyl group as this elemental step could be considered as active precursor for both MOR and poisoning process. It is widely accepted that the oxidation of CHO_{ads} in presence of adsorbed hydroxyl group (HO_{ads}) would lead to the formation of carbon dioxide.[14] Indeed, the high surface coverage of HO_{ads} becomes crucial to prioritize MOR pathway. In order to enable CO tolerance and promote MOR, many efforts have been made to control the crystallographic structure of platinum by alloying PtNPs with other metals (Ru, Au, Pd, Ni, Co, Cu, Fe)[40–42] or dispersing them on various supports (activated carbon, conducting polymers, or carbonaceous materials).[9,13,14]

MOR on PtNPs/4-ATP modified GCE was recorded using cyclic voltammetry technique in 0.5 M NaOH solution containing 0.1 M MeOH (Fig. 6). It can be seen that there is one anodic peak in forwards scan (I_f) at higher potentials (−250 mV) and another anodic peak in backward scan (I_b) at lower potentials (−360 mV). It is supposed that the first one is related to oxidation of methanol whereas the second one is attributed to the oxidation of carbonaceous intermediates, thus regeneration of active sites. As seen from Fig. 6, the peak current was increased by nearly 30% when 4-ATP supporting layer was present. In the same time, the ratio I_f/I_b was estimated to be 21 which is 2.1 times higher than that on PtNPs modified GCE. Salma Jadali has also reported an increase in I_f/I_b ratio by 50% on electrode surface modified with Pd/4-ATP/MWCNT/GCE.[15] Otherwise, the position of oxidation peak was also shifted by 60 mV towards more positive potentials. These results indicated that a better CO tolerance and a higher catalytic activity were obtained when 4-ATP supporting layer was introduced. It must be paid attention that no oxidation peak was observed on 4-ATP layer without PtNPs on top (Fig. 6). These observations are in accordance with those obtained when introducing PEDOT[8] or PANI-Ppy[11] as dispersion matrix for PtNPs.

The thickness of 4-ATP supporting layer and size distribution of PtNPs which are critical for MOR are strongly affected by deposition conditions. A thick organic film will probably restrict electrical conductivity of the electrode surface and decrease MOR signals, while a low coverage of 4-ATP on electrode surface will not provide enough binding sites for subsequent dispersion of metal nanoparticles.

The growth of big metal particles accompanied with their aggregation is not favourable, but probably it is needed to load metal nanoparticles at enough amount on surface to ensure

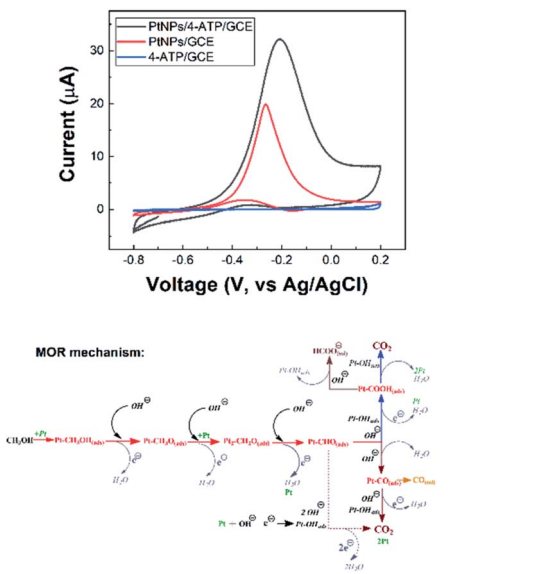

Fig. 6 MOR mechanism and enhanced MOR signal on PtNPs/4-ATP film. CV curves were recorded in 0.5 M NaOH containing 0.1 M MeOH at scan rate of 50 mV s^{-1}.

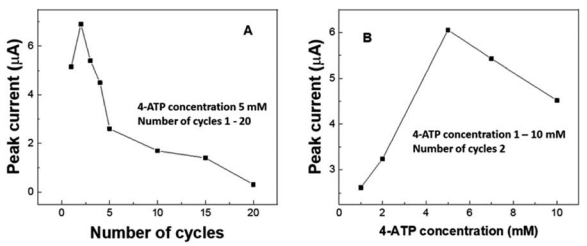

Fig. 7 Effect of grafting conditions of 4-ATP layer on MOR test. Peak current was recorded using CV technique in 0.5 M NaOH containing 0.01 M MeOH at scan rate of 50 mV s^{-1}.

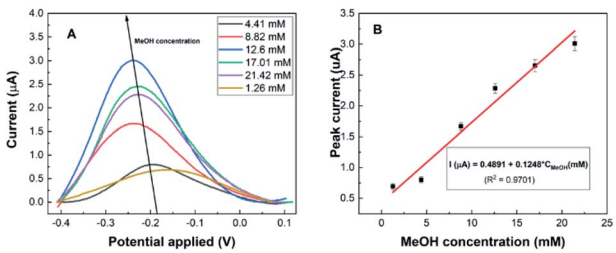

Fig. 8 MOR effect on PtNPs/4-ATP/GCE at different concentrations: (A) cyclic voltammetry curves recorded in 0.5 M NaOH solution containing MeOH at different concentrations; (B) the increase in peak current with increasing MeOH concentration.

Table 1 Comparison on MeOH sensing performances

Sensing platform	LOD (μM)	Linear range (mM)	Reference
PtNPs/4-ATP/GCE	1210	1.26–21.42	This work
PtNPs/GCE	0.6	250–1500	24
Polythiophene + α-Fe_2O_3/GCE	1590	0–1000	43
PtAuAg nanotubes/GCE	20	0.05–1.8	44

their catalytic activity. Generally, the size exceeds 30 nm is not good for catalytic activity of PtNPs.[4,24]

It must be emphasized that 4-ATP supporting layer using in this work is extremely thin compared with other conducting polymer films (hundreds of nanometers).[4–8] It is expected that the electrode surface is totally covered by a thin 4-ATP supporting layer rather than by a highly porous, thick conducting polymer film. By that way, PtNPs had opportunity to anchor and grow on a flat and adhesive substrate made of 4-ATP in order to achieve a more uniform size distribution and a higher dispersion density on electrode surface. As seen in Fig. 7, MOR test was optimized at 4-ATP concentration of 5 mM and number of scans of 2.

The onset point at which MOR starts was determined to be −495 mV. In principle, this value is related to the capability of breaking C–H bonds and the subsequent removal of intermediates generated by incomplete oxidation of methanol such as CO. The catalytic activity of a catalyst is defined as the maximum current obtained during the cyclic cycle of the methanol oxidation per weight of Pt. This value was estimated to be 200 mA mg^{-1} for PtNPs/4-ATP/GCE, which is higher than that obtained on PtNPs/GCE (133.34 mA mg^{-1}) and commercial Pt/C (169 mA mg^{-1}).[15]

It is obvious that the peak current in MOR test is increased with increasing MeOH concentration (Fig. 8B). The calibration curve was built at concentrations ranging from 1.26 to 21.42 mM. A linear relationship between MOR signal and MeOH concentration was obtained with regression equation: I (μA) = 0.48908 + 0.12476 × C (mM) (Fig. 8B). The detection limit (LOD = 3 × S_a/b on which b is the slope of regression curve and S_a is the standard deviation) was found to be 1.21 mM which is comparable with those obtained in previous works (Table 1).

3.6. Mechanism for improved MOR

The possible mechanisms for improved CO tolerance and MOR reaction is proposed as follows. The presence of free thiol groups in grafted 4-ATP supporting layer might have provided anchoring sites for high dispersion of monodisperse metal nanoparticles. In the same time, the reduction of metal salt might somehow be slowed down due to this organic barrier, and thus the particle aggregation can be avoided.[8] Besides, the adsorbed water molecules on polymeric layer might be accompanied with formation of more hydroxyl radicals which are needed to accelerate oxidation of intermediate products.[6,8] It was suggested that the organic supporting layer can be responsible to weaken Pt–CO bond either through modifying electronic structure of Pt (due to coordination between PtNPs and thiol groups) or by acting as a sink for CO due to its lipophilicity.[8,15] Lastly, the repulsive interaction between CO molecules and sulfur atoms in 4-ATP supporting layer might have limited the adsorption of CO molecules onto electrode surface, thus improved anti-poisoning activity.[15,35]

4. Conclusions

We have demonstrated an easy approach to prepare well-dispersed platinum nanoparticles with using 4-ATP thin film as supporting layer. It was found that the ratio between forward and backward current was increased by 2.1 times when 4-ATP film was introduced. The current response recorded in MOR was improved by 30% and the detection limit was as low as 1.21 mM. In our near future work, some transition metals (*i.e.*, Ni, Co) will be employed to tune electronic behavior of metal catalyst, thus enables selective detection of methanol in alcoholic mixture. Several adherent layers based on aromatic compounds containing various functional groups (thiol, hydroxyl, amine, carboxylic) will be also developed for enrichment of certain biomolecules (*i.e.*, circulating tumor cells) for bio-sensing applications.

Author contributions

All authors have given approval to the final version of the manuscript.

Conflicts of interest

There are no conflicts to declare.

Acknowledgements

This research is funded by Vietnam National Foundation for Science and Technology Development (NAFOSTED) under grant number 103.02-2018.360.

References

1 A. Hamnett, Mechanism and electrocatalysis in the direct methanol fuel cell, *Catal. Today*, 1997, **38**, 445–457.
2 Z. A. C. Ramli and S. K. Kamarudin, Platinum-Based Catalysts on Various Carbon Supports and Conducting Polymers for Direct Methanol Fuel Cell Applications: A Review, *Nanoscale Res. Lett.*, 2018, **13**, 410.
3 L. Zhao, J. P. Thomas, F. H. Nina, M. Abd-Ellah, X. Wang and K. T. Leung, Au-Pt alloy nanocatalysts for electro-oxidation of

methanol and their application for fast-response non-enzymatic alcohol sensing, *J. Mater. Chem. C*, 2014, **2**, 2707–2714.

4 S. Dominguez-Dominguez, J. Arias – Pardilla, A. Berenguer-Murcia, E. Morallon and D. Cazorla-Amoros, Electrochemical deposition of platinum nanoparticles on different carbon supports and conducting polymers, *J. Appl. Electrochem.*, 2008, **38**, 259–268.

5 M. Yaldagard, M. Jahanshahi and N. Seghatoleslami, Pt catalysts on PANI coated WC/C nanocomposites for methanol electro-oxidation and oxygen electro-reduction in DMFC, *Appl. Surf. Sci.*, 2014, **317**, 496–504.

6 O. Karatepe, Y. Yildiz, H. Pamuk, S. Eris, Z. Dasdelen and F. Sen, Enhanced electrocatalytic activity and durability of highly monodisperse Pt@PPy-PANI nanocomposites as a novel catalyst for the electro-oxidation of methanol, *RSC Adv.*, 2016, **6**, 50851.

7 H. Wu, T. Yuan, Q. Huang, H. Zhang, Z. Zou, J. Zheng and H. Yang, Polypyrrole nanowire networks as anodic micro-porous layer for passive direct methanol fuel cells, *Electrochim. Acta*, 2014, **141**, 1–5.

8 V. P. Hollie, E. Ventosa, A. Colina, V. Ruiz, J. Lopez-Palacios, J. W. Andrew, S. C. S. Lai, J. V. Macpherson and P. R. Unwin, Influence of ultrathin poly-(3,4-ethylenedioxythiophene) (PEDOT) film supports on the electrodeposition and electrocatalytic activity of discrete platinum nanoparticles, *J. Solid State Electrochem.*, 2011, **15**, 2331–2339.

9 K. Ham, S. Chung and J. Lee, Narrow size distribution of Pt nanoparticles covered by an S-doped carbon layer for an improved oxygen reduction reaction in fuel cells, *J. Power Sources*, 2020, **450**, 227650.

10 P. Kanninen, N. D. Luong, H. S. Le, J. Florez-Montano, H. Jiang, E. Pastor, J. Seppala and T. Kallio, Highly active platinum nanoparticles supported by nitrogensulfur functionalized graphene composite for ethanol electro-oxidation, *Electrochim. Acta*, 2017, **242**, 315–326.

11 Na Yang, Li Li, Li Jing, W. Ding and Z. Wei, Modulating the oxygen reduction activity of heteroatom - doped carbon catalysts *via* the triple effect: charge, spin density and ligand effect, *Chem. Sci.*, 2018, **9**, 5795–5804.

12 L. Zhang, J. Niu, M. Li and Z. Xia, Catalytic mechanisms of sulfur-doped graphene as efficient oxygen reduction reaction catalysts for fuel cells, *J. Phys. Chem. C*, 2014, **118**, 3545–3553.

13 Y.-T. Kim and T. Mitani, Surface thiolation of carbon nanotubes as supports: A promising route for the high dispersion of Pt nanoparticles for electrocatalyst, *J. Catal.*, 2006, **238**, 394–401.

14 G. Chen, Z. Dai, H. Bao, L. Zhang, L. Sun, H. Shan, S. Liu and F. Ma, Enhanced anti-CO poisoning of platinum on mesoporous carbon spheres by abundant hydroxyl groups in methanol electro-oxidation, *Electrochim. Acta*, 2020, **336**, 135751.

15 M. A. Kamyabi, M. K. Hashemi Heris and S. Jadali, Easy approach for decorating of poly 4-aminothiophenol with Pd nanoparticles: an efficient electrocatalysis for ethanol oxidation in alkaline media, *J. Solid State Electrochem.*, 2021, **25**, 1283–1292.

16 Md. Samim Hassan, P. Basera, S. Bera, M. Mittal, S. K. Ray, S. Bhattacharya and S. Sapra, Enhanced Photocurrent Owing to Shuttling of Charge Carriers across 4-Aminothiophenol-Functionalized MoSe2–CsPbBr3 Nanohybrids, *ACS Appl. Mater. Interfaces*, 2020, **12**, 7317–7325.

17 Y. Y. Yilmaz, E. E. Yalcinkaya, D. O. Demirkol and S. Timurde, 4-aminothiophenol-intercalated montmorillonite: Organic-inorganic hybrid material as an immobilization support for biosensors, *Sens. Actuators, B*, 2020, **307**, 127665.

18 R. P. A. Balvedi, A. C. H. Castro, J. M. Madurro and A. G. Brito-Madurro, Detection of a Specific Biomarker for Epstein-Barr Virus Using a Polymer-Based Genosensor, *Int. J. Mol. Sci.*, 2014, **15**, 9051–9066.

19 A. Üzer, Ş. Sağlam, Z. Can, E. Erçağ and R. Apak, Electrochemical Determination of Food Preservative Nitrite with Gold Nanoparticles/p-Aminothiophenol-Modified Gold Electrode, *Int. J. Mol. Sci.*, 2016, **17**, 1253.

20 W. Ahmed El-Said and J.-W. Choi, Electrochemical biosensor consisted of conducting polymer layer on gold nanodots patterned Indium Tin Oxide electrode for rapid and simultaneous determination of purine bases, *Electrochim. Acta*, 2014, **123**, 51–57.

21 A. I. Gopalan, K.-P. Lee, K. Manian Manesh, P. Santhosh, J. H. Kim and J. S. Kang, Electrochemical determination of dopamine and ascorbic acid at a novel gold nanoparticles distributed poly(4-aminothiophenol) modified electrode, *Talanta*, 2007, **71**, 1774–1781.

22 M.-B. Gholovand and A. Akbari, A sensitive electrochemical genosensor for highly specific detection of thalassemia gene, *Biosens. Bioelectron.*, 2019, **129**, 182–188.

23 A. S. Lapp, Z. Duan, N. Marcella, L. Luo, A. Genc, R. da Jan, A. I. Frenkel, G. Henkelman and R. M. Crooks, Experimental and theoretical structural investigation of AgPt nanoparticles synthesized using a direct electrochemical method, *J. Am. Chem. Soc.*, 2018, **140**, 6249–6259.

24 J.-Ju Feng, Ao-Qi Li, Ai-J. Wang, Z. Lei and J.-R. Chen, Electrodeposition of monodispersed platinum nanoparticles on a glassy carbon electrode for sensing methanol, *Microchim. Acta*, 2011, **173**, 383–389.

25 Y. Liu, G. Dincer, B. Ugo and T. P. Moffat, Self-terminating growth of platinum films by electrochemical deposition, *Science*, 2012, **338**, 1327–1330.

26 S. Brimaud and R. J. Behm, Electrodeposition of a Pt monolayer film: using kinetic limitations for atomic layer epitaxy, *J. Am. Chem. Soc.*, 2013, **135**, 11716–11719.

27 A. S. Lapp and R. M. Crooks, Multilayer electrodeposition of Pt onto 1- 2 nm Au nanoparticles using a hydride - termination approach, *Nanoscale*, 2020, **12**, 11026–11039.

28 S. Traipop, A. Yakoh, S. Jampasa, S. Chaiyo, Y. Boonyongmaneerat, J. Panpranot, P. Praserthdam and O. Chailapakul, Sequential electrodeposition of Cu–Pt bimetallic nanocatalysts on boron-doped diamond electrodes for the simple and rapid detection of methanol, *Sci. Rep.*, 2021, **11**, 14354.

29 R. S. Deinhammer, M. Ho, J. W. Andereg and M. D. Porter, Electrochemical oxidation of amine - containing compounds: A route to the surface modification of glassy carbon electrodes, *Langmuir*, 1994, **10**, 1306–1313.

30 Y. L. MacCarley and A. J. Bard, Scanning tunneling microscopy studies of gold (111) derivatized with organothiols, *J. Phys. Chem.*, 1992, **96**(18), 7416–7421.

31 B. I. Rosario-Castro, E. R. Fachini, J. Hernandez, M. E. Perez-Davis and C. R. Cabrera, Electrochemical and surface characterization of 4-aminothiophenol adsorption at polycrystalline platinum electrodes, *Langmuir*, 2006, **22**(14), 6102–6108.

32 L. Genies, R. Faure and R. Durand, Electrochemical reduction of oxygen on platinum nanoparticles in alkaline media, *Electrochim. Acta*, 1998, **44**, 1317–1327.

33 P. Leuaa, D. Priyasarshani, A. K. Tripathi and M. Neergat, Internal and external transport of redox species across the porous thin-film electrode/electrolyte interface, *J. Phys. Chem. C*, 2019, **123**, 21440–21447.

34 T. N. N. Dau, V. H. Vu, T. T. Cao, Van C. Nguyen, C. T. Ly, D. L. Tran, T. T. N. Pham, N. T. Loc, B. Piro and T. T. Vu, In-situ electrochemically deposited Fe_3O_4 nanoparticles onto graphene nanosheets as amperometric amplifier for electrochemical biosensing applications, *Sens. Actuators, B*, 2019, **283**, 52–60.

35 C. Retna Raj, F. Kitamura and T. Ohsaka, Electrochemical and *in Situ* FTIR spectroscopic investigation on the electrochemical transformation of 4-aminothiophenol on a gold electrode in neutral solution, *Langmuir*, 2001, **17**, 7378–7386.

36 Z.-P. Liu and P. Hu, General rules for predicting where a catalytic reaction should occur on metal surfaces: A density functional theory study of C-H and C-O bond breaking/making on flat, stepped, and kinked metal surfaces, *J. Am. Chem. Soc.*, 2003, **125**(7), 1958–1967.

37 G. S. Parkinson, Single-atom catalysis: How structure influences catalytic performance, *Catal. Lett.*, 2019, **149**, 1137–1146.

38 I. T. McCrum, C. J. Bondue and M. T. M. Koper, Hydrogen-induced step-edge roughening of platinum electrode surfaces, *J. Phys. Chem. Lett.*, 2019, **10**(21), 6842–6849.

39 D. Cao, G. Q. Lu, A. Wieckowski, S. A. Wasileski and M. Neurock, Mechanisms of methanol decomposition on Platinum: A combined experimental and *ab Initio* approach, *J. Phys. Chem. B*, 2005, **109**(23), 1133.

40 M. Rashid, J. Tae-Sun, Y. Jung and Y. S. Kim, Bimetallic core-shell Ag@Pt nanoparticle-decorated MWNT electrodes for amperometric H_2 sensors and direct methanol fuel cells, *Sens. Actuators, B*, 2015, **208**, 7–13.

41 H. Burhan, H. Ay, E. Kuyuldar and F. Sen, Monodisperse Pt-Co/GO anodes with varying Pt:Co ratios as highly active and stable electrocatalysts for methanol electrooxidation reaction, *Sci. Rep.*, 2020, **10**, 6114.

42 M. Farsadrooh, M. Noroozifar and A. R. Modarresi-Alam, An easy and eco-friendly method to fabricate three-dimensional Pd-M (Cu, Ni) nanonetwork structure decorated on the graphene nanosheet with boosted ethanol electrooxidation activity in alkaline medium, *Int. J. Hydrogen Energy*, 2019, **44**(54), 28821–28832.

43 F. A. Harraz, M. Faisal, M. Jalalah, A. A. Almadiy, S. A. Al-Sayari and M. S. Al-Assiri, Conducting polythiophene/α-Fe_2O_3 nanocomposite for efficient methanol electrochemical sensor, *Appl. Surf. Sci.*, 2020, **508**, 145226.

44 Q. Qiu, N. Jiang, L. Ge, X. Li and X. Chen, The electrochemical sensor for methanol detection based on trimetallic PtAuAg nanotubes, *J. Mater. Sci*, 2020, **55**, 15681–15694.